UC Irvine
Faculty Publications

Title
Regional calibration of coral-based climate reconstructions from Palau, West Pacific Warm Pool (WPWP)

Permalink
https://escholarship.org/uc/item/4ms7q9ff

Journal
Palaeogeography, Palaeoclimatology, Palaeoecology, 386

ISSN
00310182

Authors
Osborne, Michael C
Dunbar, Robert B
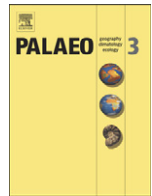Mucciarone, David A
et al.

Publication Date
2013-09-01

DOI
10.1016/j.palaeo.2013.06.001

Regional calibration of coral-based climate reconstructions from Palau, West Pacific Warm Pool (WPWP)

Michael C. Osborne [a,*], Robert B. Dunbar [a], David A. Mucciarone [a],
Joan-Albert Sanchez-Cabeza [b,c], Ellen Druffel [d]

[a] Department of Environmental Earth System Science, Stanford University, Stanford, CA, 94305-4216, USA
[b] Institut de Ciència i Tecnologia Ambientals, Departament de Física, Universitat Autònoma de Barcelona, 08193 Bellaterra, Spain
[c] Instituto de Ciencias del Mar y Limnología, Universidad Nacional Autónoma de México, 04510 Ciudad de México, D.F., Mexico
[d] Department of Earth System Science, University of California, Irvine, Irvine, CA 92697-3100, USA

ARTICLE INFO

ABSTRACT

Stable isotopic and trace element records from corals collected within the West Pacific Warm Pool (WPWP) are well suited to examine interannual to decadal climate variability associated with the El Niño-Southern Oscillation (ENSO) phenomenon. The most commonly used climate recorder in corals is $\delta^{18}O$ ($\delta^{18}O_{CRL}$), a parameter subject to multiple regional and local environmental influences. Location-specific calibration of $\delta^{18}O_{CRL}$ is a necessary first step for developing long-term paleoceanographic reconstructions. Here we present four new coral $\delta^{18}O$ stratigraphies from the Republic of Palau (7.5°N 134.5°E), and compare our records with instrumental measurements for the period 1950–2008. We also compare our results with a previously published coral record from Palau. We employ a new sea surface salinity (SSS) product and validate its utility for coral-based paleoclimate calibrations. We not only examine differences among the records but also identify strong and regionally coherent environmental signals. We find that SSS variability is the dominant influence on $\delta^{18}O_{CRL}$ in Palau, while sea surface temperature (SST) is of secondary importance. Our results show that time-averaging multiple $\delta^{18}O_{CRL}$ records into a single composite series produce greater correlations with instrumental data and indices than individual stratigraphies alone. Our results are consistent with observations of a strengthening of the hydrological cycle in the WPWP region over the past 50 years, though the magnitudes of long term linear trends differ among the different Palau $\delta^{18}O_{CRL}$ records. Interannual and interdecadal variabilities between the Palau $\delta^{18}O_{CRL}$ records are more consistent than the long term linear trends. Monthly Palauan $\delta^{18}O_{CRL}$ anomalies capture strong El Niño events with high fidelity over the calibration period. This study provides constraints for future paleoenvironmental investigations in Palau using longer coral records.

1. Introduction

The West Pacific Warm Pool (WPWP) is a broad region in the tropical Pacific characterized by mean annual SSTs greater than 28 °C (Wyrtiki, 1989). WPWP heat storage is significant as atmospheric convection and associated precipitation is enhanced at such high temperatures (Graham and Barnett, 1987; Picaut et al., 1996). On interannual time scales, precipitation anomalies over the WPWP are tightly linked with El Niño-Southern Oscillation (ENSO) variability through atmospheric teleconnections and shifting Walker circulation. Climate anomalies associated with ENSO are global in nature, and there is great interest in predicting the evolution of ENSO under greenhouse forcing (Chen et al., 2004; Collins et al., 2010). Moreover,

in recent decades the WPWP has experienced a shift towards warmer and fresher surface waters, a trend that has consequences for the future of ENSO dynamics (Maes et al., 2005; Cravatte et al., 2009; Durack and Wijffels, 2010; Durack et al., 2012). However it is unclear whether recent changes in the WPWP have an anthropogenic footprint or are part of natural variability (Collins et al., 2010).

Instrumental records from the tropical Pacific are limited before ~1950, inhibiting our understanding of ENSO variability on decadal to centennial time scales. As a result, the tropical Pacific has been a target region for high resolution paleoceanographic studies (Cole et al., 1993; Dunbar et al., 1994; Tudhope et al., 1995; Quinn et al., 1998; Dunbar and Cole, 1999; Gagan et al., 2000; Urban et al., 2000; Evans et al., 2002; Hendy et al., 2002; Quinn and Sampson, 2002; Cobb et al., 2003; Asami et al., 2005). Scleractinian coral records are particularly well suited to address past modes of ENSO behavior, as they often span several decades to centuries at sub-seasonal to monthly resolution (Corrège, 2006). However, coral $\delta^{18}O$ records are often difficult to interpret, as a variety of both correlated and

* Corresponding author at: Environmental Earth System Science, 473 Via Ortega, Rm 140, Stanford, CA 84305-4216, USA. Tel.: +1 650 644 6695; fax: +1 650 498 5099.
E-mail address: osbornemc@gmail.com (M.C. Osborne).

independent environmental variables can contribute to changes in isotopic composition.

$\delta^{18}O_{CRL}$ is a function of the isotopic composition of the surrounding seawater ($\delta^{18}O_{SW}$), the temperature-dependent fractionation of $^{18}O/^{16}O$ ratio of the mineral aragonite, and biological kinetic disequilibrium offsets referred to as 'vital effects' (Weber and Woodhead, 1972; Cohen and McConnaughey, 2003; McConnaughey, 2003; Sinclair, 2005; Juillet-Leclerc et al., 2009; Krief et al., 2010; Mizrachi et al., 2010). Empirical studies generally demonstrate a linear relationship between $\delta^{18}O_{SW}$ and SSS, but this relationship is subject to regional differences. For example, Fairbanks et al. (1997) calculated a slope of 0.27‰/psu using a network of tropical Pacific sites, while Morimoto et al. (2002) derived a value of 0.42‰/psu from in situ calibration in Palau. Note that we use practical salinity units (psu) in order to be consistent with available SSS data (see Section 3.2), while recognizing that the new standard for salinity units is absolute salinity (Millero et al., 2008). In general, the ability to parameterize the $\delta^{18}O_{SW}$–SSS relationship is difficult because direct $\delta^{18}O_{SW}$ measurements are sparse (LeGrande and Schmidt, 2006; Linsley et al., 2008). In addition, calibration studies have shown that the slope of the temperature dependence is not always constant, even for a given

genus (Weber and Woodhead, 1972; Grottoli and Eakin, 2007). Additional complicating factors arise from local environmental influences such as bio-erosion, variable extension/calcification rates, depth of coral colony, and fish grazing (Linsley et al., 1999; Felis et al., 2003).

The Republic of Palau is located within the northwestern portion of the WPWP (Fig. 1). The WPWP experiences large precipitation anomalies in response to interannual ENSO variability. In contrast to the eastern Pacific, dry conditions and slight cooling occur in the WPWP during ENSO warm phases, while wet and warm conditions accompany ENSO cool phases. This climatic forcing exerts an additive effect on $\delta^{18}O_{CRL}$ (Guilderson and Schrag, 1999; Urban et al., 2000). Previous paleoceanographic studies from Palau demonstrate potential for coral and sclerosponge records to capture ENSO variability (Morimoto et al., 2002; Iijima et al., 2005; Grottoli, 2006; Grottoli et al., 2010; Wu and Grottoli, 2010). Morimoto et al. (2002) conducted a two-year calibration study of $\delta^{18}O_{CRL}$ in Palau, and Iijima et al. (2005) subsequently generated a 45-year coral record. However, the reproducibility of these coral records has not previously been evaluated. More recently, Grottoli et al. (2010) published a 55-year sclerosponge record from an open ocean site in eastern Palau. While sclerosponges represent a promising new signal carrier for paleoceanographic investigations,
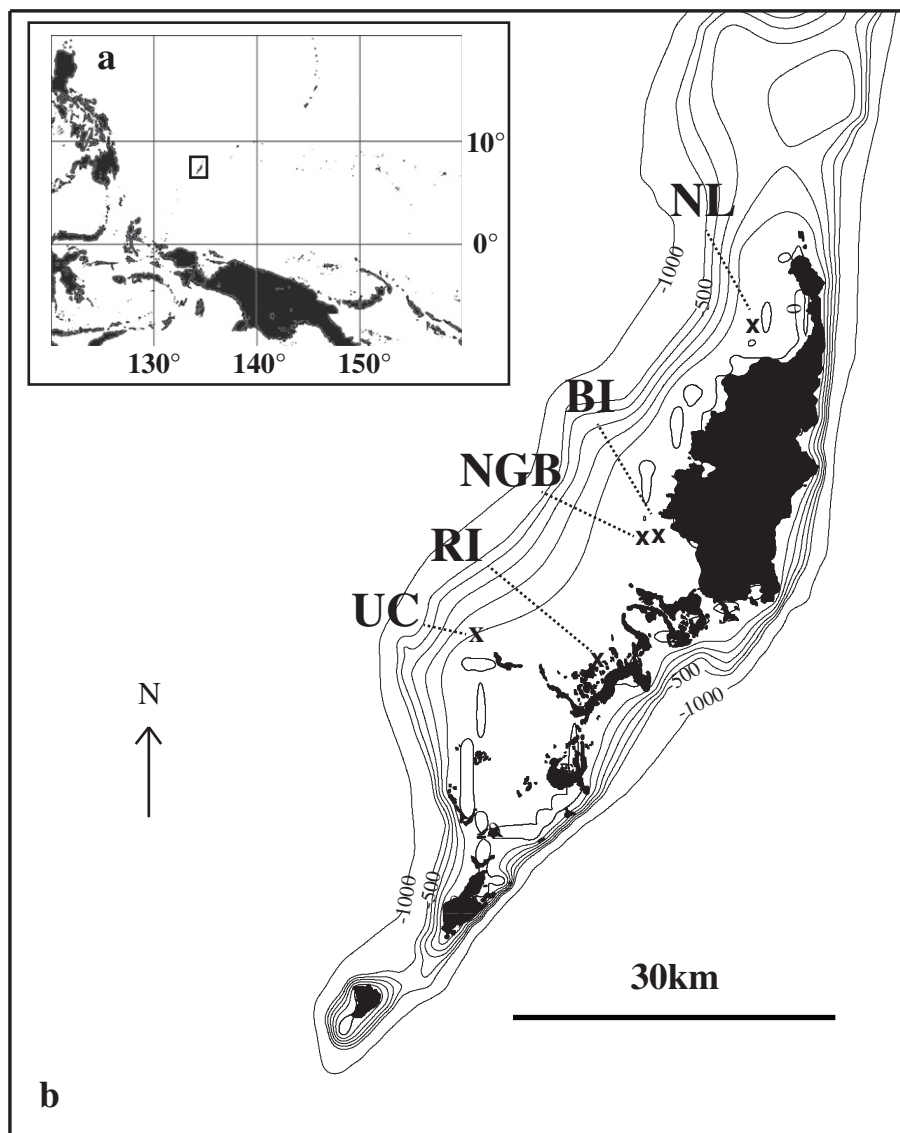
Fig. 1. a) Regional map of the field. Stippled box indicates study site. b) Enlargement of coral collection sites. Site abbreviations are as follows: Ulong Channel (UC), Ngaragabel (NGB), Ngeralang (NL), Rock Islands (RI), and Babeldaob Island (BI, sampled by Iijima et al., 2005). Subsurface contours in 100 m intervals.

questions remain regarding sampling strategy and age model construction (Swart et al., 1998; Rosenheim and Swart, 2007; Wu and Grottoli, 2010).

Here we present four new coral stable isotope records from Palau and compare our results to a previously published $\delta^{18}O_{CRL}$ record (Iijima et al., 2005) as well as instrumental data. Our study is unique in that these new records complement existing stratigraphies and come from a broad range of shallow water environments within Palau. By sampling multiple sites we are able to test the degree to which local effects such as limited water mass exchange and coral colony depth result in divergences between records. This approach, suggested by Linsley et al. (1999), represents one strategy for evaluating the fidelity of coral-based paleo-records. The present study also validates the use of a gridded SSS dataset recently made available by the French Sea Surface Salinity Observation Service (hereafter LEGOS SSS; http://www.legos.obs-mip.fr/observations/sss/; Asami et al., 2004; Delcroix et al., 2011). Finally, we compare the $\delta^{18}O$ records to the Multivariate ENSO Index (MEI), and discuss the conformity of coral records with recent warming and freshening trends across the WPWP (Wolter and Timlin, 1993, 1998; Grottoli and Eakin, 2007; Cravatte et al., 2009; Durack et al., 2012).

2. Study area

2.1. Oceanographic setting

The Palau archipelago lies at a crossroads of oceanic currents between the Philippine Sea and the Pacific (Fig. 1a); the westward flowing North Equatorial Current drives much of the surface flow, while the eastward flowing North Equatorial Countercurrent lies further south. The strength and position of both currents vary seasonally (Fine et al., 1994). Transient and non-stationary eddies, such as the Mindanao and the Halmahera eddies, significantly influence the mean oceanography (Heron et al., 2006; Wolankski and Furukawa, 2007). Overall these general circulation patterns exhibit large interannual variability and regional circulation is greatly altered during ENSO events (Fine et al., 1994; Wolankski and Furukawa, 2007). For example, Wolankski and Furukawa (2007) document a gradual cessation of surface currents from April 2008 to July 2008, resulting in a deeper thermocline and increased SSTs in the waters surrounding Palau. This period also coincided with mass coral bleaching in Palau (Bruno et al., 2001).

2.2. Coral sampling sites

Coral cores were collected in November 2008 from massive *Porites lutea* colonies at four sites, shown in Fig. 1b along with the locations of the previously published $\delta^{18}O_{CRL}$ record (Iijima et al., 2005). Ulong Channel (UC) is located along the outer reef margin facing the Philippine Sea and experiences strong tidal exchange with the open ocean and isolation from terrestrial input. In contrast, the Ngeragabel (NGB), Ngeralang (NL), and Babeldaob Island (BI, sampled by Iijima et al., 2005) are lagoon sites in near-shore waters. The Rock Islands (RI) site is situated in a restricted embayment (see Appendix Fig. A.1). Circulation within lagoons and embayments varies as a function of tides, winds, and regional currents, and the residence time of waters is likely variable between sites (Wolankski and Furukawa, 2007; Colin, 2009).

3. Materials and methods

3.1. Isotope analyses and chronology

Large colonies of the massive coral *Porites lutea* were sampled using a 3-inch underwater hydraulic drill. Cores were sectioned into slabs 7 cm wide and 7 mm thick using a diamond blade tile saw.

Slabs were then cleaned with DI water, dried, and X-rayed in order to reveal growth (density) banding (Fig. 2). We extracted aragonite powder by milling 3 mm wide × 2 mm deep trenches at 1 mm increments down-core along growth axes using a Dremel Tool drill with a 0.5 mm drill bit. Powders were analyzed for $\delta^{18}O$ and $\delta^{13}C$ VPDB using a Finnigan MAT 252 and Kiel III acidification device at the Stanford University Stable Isotope Lab (SIBL). 10% of all coral samples were replicated, and the precision estimate based on coral replicates is ± 0.05‰ for $\delta^{18}O$ and ± 0.06‰ for $\delta^{13}C$ (mean $\pm$ SD). Precision based on replicate analysis of an in-house lab standard (6 per wheel of 40 unknowns) is ± 0.05‰ for $\delta^{18}O$ and ± 0.04‰ for $\delta^{13}C$.

3.2. Environmental data

We use several instrumental products to calibrate the Palau records. Since 2001, Onset Hobo Pro-8 recording thermisters with an accuracy of 0.1 °C have been deployed at Ulong Channel at a depth of 11 m, providing in situ measurements (P. Colin, personal communication) (Fig. 3b). We correlated this in situ temperature data with the NCEP-NCAR reanalysis product for 2000–2008 (obtained by centering a 1° × 1° grid over Palau; available at http://www.esrl.noaa.gov/; Kalnay et al., 1996), and found r = 0.87 (p < 0.01). The mean difference between the NCEP-NCAR and in situ SST is ~0.27 °C, with the in situ data displaying slightly cooler temperatures. With one exception in early 2003, the maximum difference is <1 °C (Fig. 3b). Based on this validation of the reanalysis data for calibrating a coral isotope record in Ulong Channel, we use NCEP-NCAR SST data for the period 1970 to 2008. Over this period, average SST in Palau is 28.7 ± 0.6 °C (mean ± SD) and exhibits limited seasonal variability (Fig. 3a). The mean annual difference between monthly maxima and minima SST is ~1.6 ± 0.4 °C. The monthly SST climatology shows ~28.0 ± 0.4 °C minima in Feb/March. The SST data show warming of ~0.5 °C since 1970.

We use salinities derived from a new SSS gridded dataset (Delcroix et al., 2011). The LEGOS SSS product is generated by aggregating in situ observations from moored buoys, CTD casts, Argo floats, research vessels and ships of opportunity (Delcroix et al., 2011). The associated uncertainties reflect transient and dispersed sampling. As with the NCEP-NCAR SST data, the SSS time series was extracted by centering a 1° × 1° grid over Palau (Fig. 3c). We correlated the LEGOS SSS with the Simple Ocean Data Assimilation (SODA) reanalysis data set, and found r = 0.48 (p < 0.01) (Carton and Giese, 2008). We chose to use the LEGOS product because multiple ships of opportunity traverse the waters surrounding Palau (Delcroix et al., 2011; Gorman et al., 2012). SSS uncertainties are relatively high in the LEGOS SSS pre-1970, so we only include this time series from 1970 to 2008. The LEGOS SSS climatology shows maxima of 34.2 psu (SD = ~0.2 psu) in Feb/March. The mean annual difference between monthly maxima and minima SSS is 0.49 ± 0.17 psu. SSS anomalies >0.34 psu (exceeding 2 standard deviations from the annual mean) appear only during periods of extreme ENSO warm events. The SSS data display a long term freshening of ~0.3 psu.

Monthly mean precipitation rates have been recorded intermittently at Koror airport since 1925. Fig. 3d shows the precipitation anomaly record relative to the series mean since 1970 (obtained from the GHCN v2 at the IRI/LDEO Climate Data Library, http://iridl.ldeo.columbia.edu; Xie and Arkin, 1997). There is no clear long-term trend in the precipitation data. However, the Koror precipitation record displays anomalously low values during the 1972/73, 1982/83, and 1997/98 ENSO warm events.

Fig. 4 shows a plot of the SST$_{ANOM}$ and the SSS$_{ANOM}$ with the MEI for the period 1970–2008. The anomaly time series were generated using the period 1970–2000 as a climatological base period. All time series have been detrended and normalized to unit variance. In this report we employ the MEI as a comparative index for ENSO activity, because the MEI incorporates multiple climate variables from across the tropical
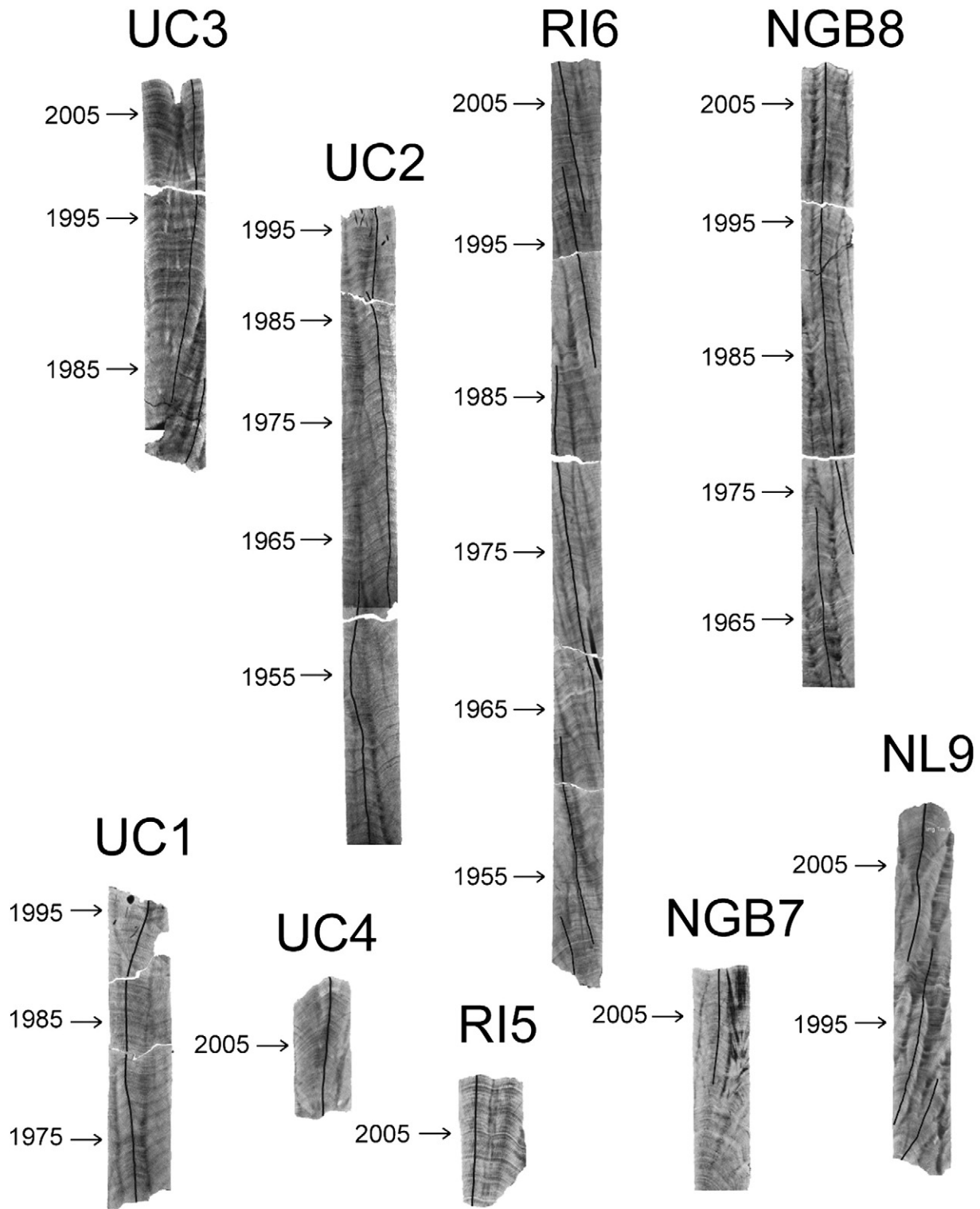
Fig. 2. Coral positive x-radiographs. Abbreviations are as follows: UC = Ulong Channel, RI = Rocks Islands, NGB = Ngeralang, NL = Ngeralang. Numbers following acronyms correspond to separate cores at each site. Sample paths are indicated by black lines.

Pacific basin. The MEI also correlates strongly with SST variability in the Niño 3.4 region (Wolter and Timlin, 2011). The SSS_{ANOM}-MEI correlation ($r = 0.54$) is greater than the SST_{ANOM}-MEI correlation ($r = -0.29$), consistent with the view that hydrologic variation is the dominant climate response to ENSO forcing in this sector of the tropical Pacific (Grottoli, 2006; Grottoli et al., 2010). In particular, the SSS_{ANOM} time series captures the strong ENSO warm events of 1972/73, 1982/83, and 1997/98. For these three events, peak SSS anomalies appear

1–3 months following peak MEI anomalies. Since these correlations were determined at monthly resolution, the moderate SSS_{ANOM}-MEI correlation is likely attributable to the variable lagged climatic response.

3.3. Coral chronology

In order to make direct comparison with monthly instrumental data, age models were constructed through the combined use of
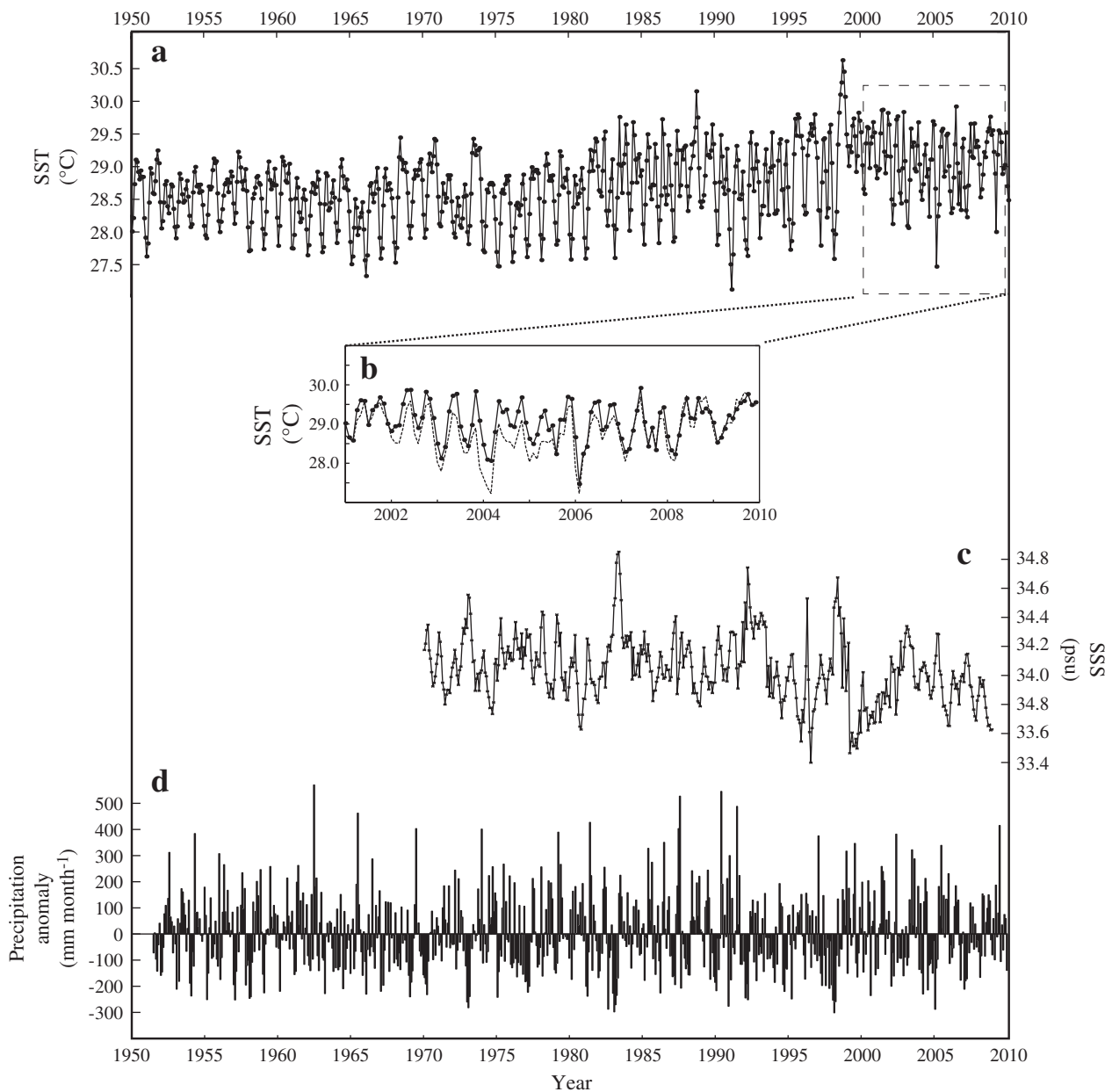
Fig. 3. Time series of instrumental records from 1970–2008 a) NCEP-NCAR SST since (black). b) Expanded view for the period of overlap between NCEP-NCAR (black, dotted) and P. Colin in situ (gray, stippled) SST since 2001. c) LEGOS SSS. d) Koror airport precipitation anomaly relative to the mean precipitation for 1970–2000.

growth bands (assumed to be annual in nature) and seasonal stable isotope variations. In general, $\delta^{18}O_{CRL}$ minima occur within denser seasonal bands (brighter regions of the coral X-ray positives). Density bands are obscure in some sections, a possible result of the weak seasonality in Palau. However, strong seasonal variations in $\delta^{18}O$ and $\delta^{13}C$ were present throughout the sampled transects. In order to convert isotope samples to a monthly resolution time series, we associated each seasonal $\delta^{18}O_{CRL}$ maxima with March, which is the month of climatological maxima in SSS and near minima in SST. We then applied a linear interpolation of $\delta^{18}O$ between annual anchor points to create a resampled times series of 12 samples/yr (out of an original time series that averages 14–20 samples/yr, depending on the mean growth rate for each colony). We experimented with using February as the anchored month, and these modifications did not significantly alter our results. We also experimented with adding additional age-control points for each year by anchoring $\delta^{18}O_{CRL}$ minima to the monthly SST maximum/SSS minimum. However, applying two

anchors per year was problematic, because the mean seasonal signal in SSS and SST during warmer/wetter months is inconsistent from year to year. For example, SSS reaches a mean seasonal minimum in October, and mean seasonal SST is ~29.3° in both June and November. We therefore concluded that a single chronological tie point per year introduces less bias when applying regression analyses.

The record from UC presented here is based on a two-colony spliced composite from this site for the period 1970–2008. As noted in Table 1, four *Porites* cores were sampled at the UC site. Two of the cores were sampled from live colonies, and two cores were sampled from a colony that died during the 1998 mass-bleaching event (P. Colin, personal communication). We denote the two cores from the dead colony as UC1 and UC2, and the two cores from the live colony as UC3 and UC4. After applying our age-model, we observed an offset between UC2 and the remaining specimens from this site for the period between 1984 and 1996 (Fig. 5a). There is a general agreement of results for cores UC1, UC2 and UC3 pre-1983 (U4 does
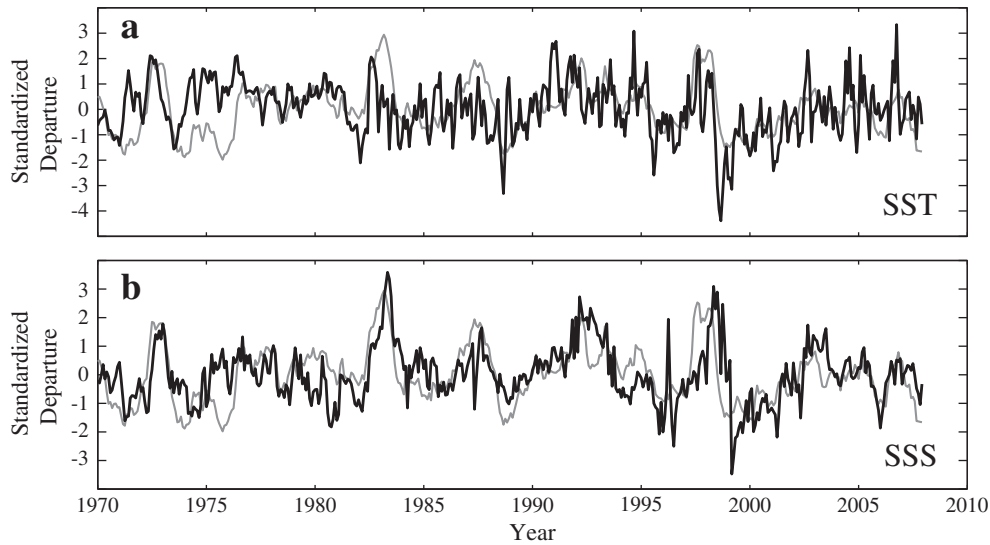
Fig. 4. Detrended instrumental anomaly records (black) with MEI (gray) for 1950–2008. a) NCEP-NCAR SST. Note SST has been inverted for visual comparison. b) LEGOS SSS.

not extend beyond 2003). The observed divergence in core UC2 corresponds to a depth of ~20 cm from the top of the core. We speculate that the uppermost section of UC2 underwent significant bio-erosion over the 10-year period between mortality and collection, leading to spurious $\delta^{18}O_{CRL}$ values near the top portion of the record. Since UC1, UC2 and UC3 converge pre-1983, we chose to use the $\delta^{18}O_{CRL}$ results from UC2 for portions that precede the 82/83 ENSO event. We averaged the three records during the 82/83 ENSO warm event, and used the $\delta^{18}O_{CRL}$ results from UC3 for the remainder of the UC record. For the RI and NGB we observed excellent agreement between colony companion cores (Fig. 5b and c). With the exception of UC2, no growth hiatuses were observed in any of the other coral records and our selection of sampling transects was facilitated by unambiguous growth habit. Our analyses of $\delta^{13}C$ variability were inconclusive, and we therefore refrain from further interpretations of $\delta^{13}C$ variability in this report. All $\delta^{18}O$ and $\delta^{13}C$ records are available at the NOAA paleoclimate database (http://www.ncdc.noaa.gov/paleo/paleo.html).

4. Results

### 4.1. Correlations between $\delta^{18}O$ and environmental records

Fig. 6a–d shows the time series of all Palau $\delta^{18}O$ records and corresponding coral growth (linear extension) rates for each site. Table 2 lists a summary of $\delta^{18}O$ statistics for the period between 1950 and 2008. For the previously unpublished records, mean $\delta^{18}O_{CRL}$ are −5.79‰ for RI and −5.50‰ for NGB, a difference of 0.29‰. The

standard deviation of the computed monthly time series for all coral records ranges from 0.16 to 0.21‰. We estimated the annual $\delta^{18}O_{CRL}$ range by subtracting each annual maximum from the minimum for all years. The mean annual range in $\delta^{18}O_{CRL}$ ranges from 0.41 to 0.48‰. We estimated the average extension rate by measuring the sample distance between chronology tie-points, and verified our results via visual inspection of the coral X-rays (Fig. 2). RI has the largest extension rate (20.5 ± 3.3 mm/yr), and UC the slowest (13.6 ± 2.0 mm/yr) (mean ± SD).

Table 3a lists the Pearson-Product Correlation matrix between all the records and instrumental data for the period 1970–2008. NL does not extend before 1990, so we excluded it from this analysis. Following the calibration strategy of Linsley et al. (1999), we generated a 3 coral composite by averaging all of the monthly resolved coral records for this period into a single composite time series (i.e., UC, RI, and NGB). UC and RI are the two most closely correlated time series (r = 0.63, p < 0.01). As expected from environmental considerations, all records display positive $\delta^{18}O$–SSS correlations and negative $\delta^{18}O$-SST correlations. We removed the annual cycle by converting the instrumental and $\delta^{18}O$ records into monthly anomaly time series ($\delta^{18}O_{ANOM}$) using 1970–2000 as a climatology base period (Appendix Table A.1a). The $\delta^{18}O_{ANOM}$ time series was not detrended. We then repeated our correlation analyses. Notably, all records show a stronger correlation to SSS than to SST in both the original and the anomaly records. In addition, the correlations between the 3 coral composite and the instrumental data are stronger than any of the correlations present in the individual records. The correlations between the

Table 1
Summary of records used in this study.

Site	Species	# of collected specimens (cores)	Lat/long position	Collection depth (m)	Brief site description
Ulong Channel (UC)	*Porites lutea*	4	7°17.153″N 134°15.016″E	12	Western Palau, Open Ocean, fringing reef, minimal terrestrial inputs
Rock Islands (RI)	*Porites lutea*	2	7°16.248″N 134°23.024″E	2	Western Palau, soft reef, restricted embayment with terrestrial inputs likely
Ngaragabel (NGB)	*Porites lutea*	2	7°24.386″N 134°26.115″E	3	Western Palau, Open lagoon, patch reef,~6.5 km from land, and ~9.5 km from open ocean
Ngeralang (NL)	*Porites lutea*	1	7°39.413″N 134°33.907″E	3	Western Palau, Open lagoon, patch reef,~4.3 km from land, and ~3 km from open ocean
Baebeldaod Island (BI; Iijima et al. 2005)	*Porites* sp.	2	7°24.505″N 134°26.115″E	3	Western Palau, Open lagoon, ~5.0 km from land, and ~11.0 km from open ocean
Short Drop Off (SDO; Grotolli et al., 2010)	*Acanthocheatetes wellsi*	1	7°16′N 134°31′E	17	Eastern Palau, open ocean, >5 km from nearest island, minimal terrestrial input
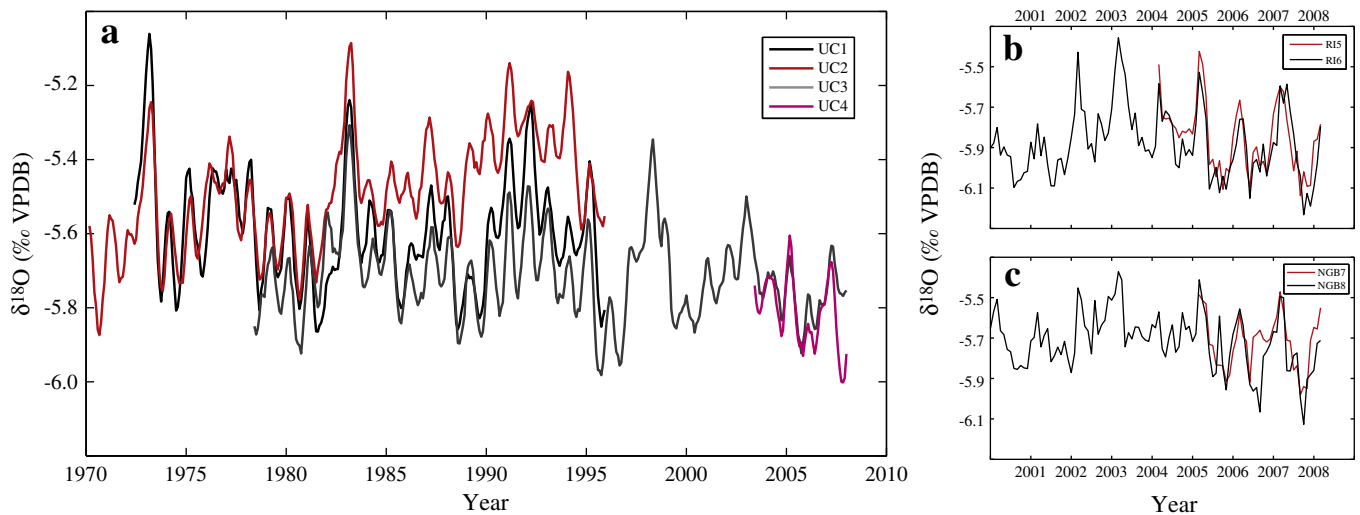
Fig. 5. Colony companion time series of all $\delta^{18}O_{CRL}$ records a) Ulong Channel (UC). UC1 (black) & UC2 (red) were collected from the same deceased colony. UC3 (gray) & UC4 (pink) were collected from the same living colony. All UC time series have been smoothed with a 5-month running mean. b) RI5 (black) & RI6 (red) collected from the same living colony. c) NGB7 (red) & NGB8 (black) collected from the same living colony.

Palau $\delta^{18}O$ records and instrumental data using monthly anomalies are reduced compared with the original time series.

In order to compare the new $\delta^{18}O$ records with the previously published BI record (Iijima et al., 2005), we repeated the correlation analyses using both the original and the anomaly time series for the period 1970–2000 (Tables 3b and Appendix Table A.1b). All records excluding NL overlap for this period, so we generated a 4 coral composite using the BI record by averaging all monthly resolved records into a single time series. Qualitatively, the results in Table 3a are similar to the results displayed in Table 3b. The $\delta^{18}O$–SSS correlations are higher in both the original and anomaly records. Small errors in age assignments have the potential to degrade our correlation coefficients, and we therefore experimented with correlation analyses at different resolutions (by binning monthly data into quarterly and 6-month bins) using the original time series for the period 1970 to 2000 (Appendix Table A.2). The largest change was at RI where the $\delta^{18}O$-SST correlation drops from -0.42 at monthly resolution to -0.18 at annual resolution. However, most of the differences in the coral records were minimal, and we therefore focus on the monthly resolved records.

4.2. Pseudocoral model and relative contributions of SST and SSS

In order to account for the influence of both SST and SSS on $\delta^{18}O$, we generated a pseudocoral, or model $\delta^{18}O$ stratigraphy for the Palau records (Asami et al., 2004; Brown et al., 2008; Thompson et al., 2011; Gorman et al., 2012). The pseudocoral was determined for the original monthly resolved time series. Following the strategy of Iijima et al. (2005), we combined the instrumental SSS and SST time series with regression coefficients derived by Morimoto et al. (2002):

$$\delta^{18}O_{CRL}(‰) = a_1\left(‰/°C\right)SST\left(°C\right) + a_2(‰/psu)SSS(psu) + a_3 \qquad (1)$$

where a_1 is the temperature-dependant fractionation coefficient, a_2 was determined by $\delta^{18}O_{SW}$–SSS regression, and a_3 is a constant resulting from regression analysis. In the Morimoto et al. (2002) and Iijima et al. (2005) studies, a_1 was specified at -0.189 (‰/°C) for western Pacific *Porites* corals, and a_2 was found to be 0.42 (‰/psu) by in situ $\delta^{18}O_{SW}$–SSS regression. We correlated the pseudocoral with each of the $\delta^{18}O_{CRL}$ records for the period 1970–2008. Following the approach of Gorman et al. (2012), we optimized the influence of

SSS and SST by testing the percent contribution in 1% increments for each site as well as the 3 coral composite (Appendix Table A.3). Consistent with the results in Table 3a, the SSS component was greater than the SST component in all instances. The percent contribution from SSS ranged from 56% (NGB) to 75% (RI).

### 4.3. Pseudocoral model via multiple linear regression

We noted two problems with applying the coefficients derived by Morimoto et al. (2002) directly to Eq. (1). First, we observed discrepancies between the LEGOS SSS and the SSS reported by Morimoto et al. (2002). For example, the SSS measures by Morimoto et al. (2002) ranged from 32.4 to 35.4 psu from 1998 to 2000 while the LEGOS SSS ranged from 33.4 to 34.7 psu over the same period, suggesting that the SSS values measured in the calibration study are not regionally representative. Second, the pseudocoral consistently underestimated the variance of the measured $\delta^{18}O$ time series (SD = 0.09 for pseudocoral vs. Table 2). We therefore solved Eq. (1) empirically by applying a multiple linear regression model using anomaly records (not detrended) for both the instrumental data and Palau $\delta^{18}O$ records (Tables 4a and 4b). We chose to perform the regressions using monthly anomalies to avoid biases due to serial autocorrelation. Regression using monthly anomalies renders $a_3 = 0$ in Eq. (1). We used the regression results to produce site-specific models for each of the $\delta^{18}O$ records, and we compare these results to measured $\delta^{18}O_{ANOM}$ (Tables 4a and 4b). Significance of the relationships was examined using two-sided Pearson's tests at 95% confidence. We performed these analyses for both calibration periods (1970–2008 and 1970–2000) in order to include BI. For the calibration period 1970–2008, correlations between the model and measured values for $\delta^{18}O_{ANOM}$ are strongest for the 3 coral composite (r = 0.75, p < 0.01), and weakest for RI (r = 0.57, p < 0.01). For the calibration period 1970–2000, correlations between the model and measured values for $\delta^{18}O_{ANOM}$ are strongest for the 4 coral composite (r = 0.77, p < 0.01), and weakest for RI (r = 0.51, p < 0.01).

5. Discussion

5.1. Relation between coral and environmental variables

The most important feature of our analyses is the consistency with which the coral records track the interannual variability present in the instrumental observations, despite notable differences between
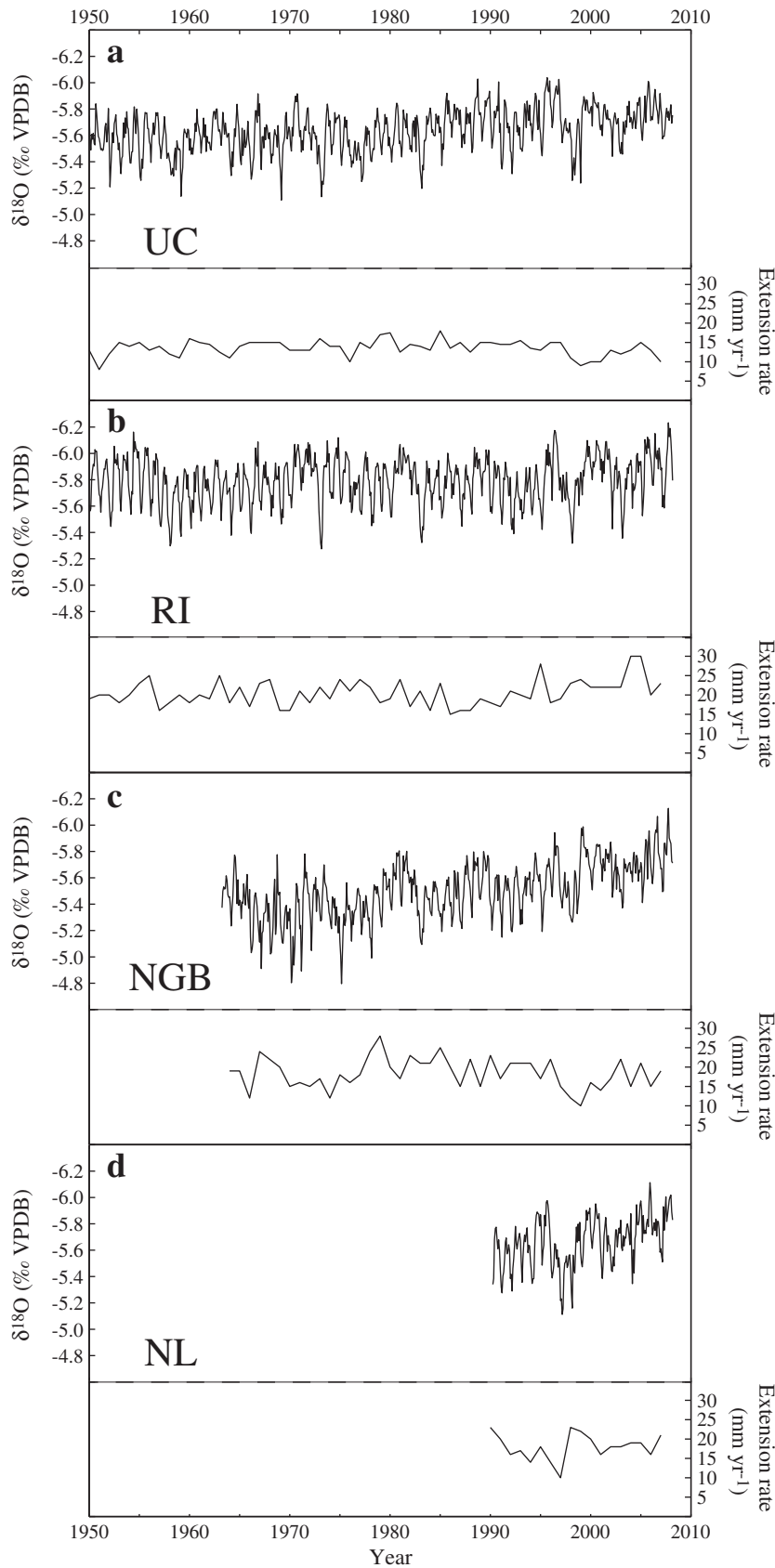
Fig. 6. Time series of all Palau δ¹⁸O records along with corresponding extension rates for each record from 1950 to 2008. a) Ulong Channel. b) Rock Islands. c) Ngaragbel. d) Ngeralang.

the four new $\delta^{18}O_{CRL}$ stratigraphies. For example, the mean $\delta^{18}O_{CRL}$ difference is as large as 0.39‰ between BI and NGB, and the correlations between the coral records range between 0.48 and 0.65

(Tables 2 and 3b). We examined systematic differences in the mean and variance of $\delta^{18}O_{CRL}$ as a function of colony depth for the period 1990–2008, and found that $\delta^{18}O_{CRL}$ variance decreased with increasing

Table 2
Summary of statistics for all records used in this study. All $\delta^{18}O$ results are reported relative to the VPDB standard. For annual range and extension rate, 1 sigma errors (1σ) are denoted in parentheses.

	UC	RI	NGB	NL	BI
Period of record	1950–2008	1950–2008	1964–2008	1990–2008	1954–2000
Sample size (n)	699	699	529	217	553
Average $\delta^{18}O$ (‰)	−5.63	−5.79	−5.50	−5.66	−5.89
$\delta^{18}O$ standard deviation (‰)	0.16	0.17	0.21	0.19	0.17
Annual range (‰)	0.41 (0.10)	0.48 (0.09)	0.47 (0.10)	0.46 (0.11)	0.41 (0.12)
Series minimum (‰)	−6.04	−6.23	−6.13	−6.11	−6.37
Series maximum (‰)	−5.03	−5.28	−4.80	−5.11	−5.42
Extension rate (mm/yr)	13.6 (2.0)	20.5 (3.3)	18.3 (3.9)	18.5 (3.3)	n/a

depth. However, we observed no systematic difference in mean $\delta^{18}O_{CRL}$ as a function of colony depth. In addition to environmental factors such as local SSS and SST, the mean difference between the sites may be a function of vital effect offsets. For the multiple regression analyses, the percentage of variance explained by SST and SSS in all individual $\delta^{18}O_{ANOM}$ records sums to less than 50%, which suggests analytical or biological noise in the data, imperfections in our age model interpolation scheme, or influences from unknown forcings. Nevertheless, the results from multiple linear regression analysis are consistent between sites (Tables 4a and 4b). We also find that $\delta^{18}O_{CRL}$ correlations with SSS are stronger than with SST in all instances, supporting previous conclusions that SSS exerts the dominant control on $\delta^{18}O_{CRL}$ in Palau in the modern climate (Morimoto et al., 2002; Grottoli et al., 2010). Detailed oceanographic data from each site is limited, though researchers engaged in monitoring coral diversity within Palau have made anecdotal observations of variable surface currents and water residence times at the four collection sites (Colin, 2009). Despite the uncertainty of local oceanographic circulation, the consistency of our results suggests that the corals from the different sites are responding to regional climate forcing, particularly at interannual timescales. Site to site differences in $\delta^{18}O_{CRL}$ stratigraphies from Palau are minimal in comparison to the regional signal.

Another salient feature of our analyses is the improvement of correlations using a 3 coral composite series, a technique suggested by Linsley et al. (1999) and verified elsewhere (Stephans et al., 2004) (Table 4a). Correlations are similarly greater for the 4 coral composite over the shorter period of analysis (Table 4b). An explanation for this improvement in correlations is that anomalous or divergent $\delta^{18}O_{CRL}$ values present in a particular record but absent in other records are minimized by time-averaging multiple stratigraphies. Local effects such as fish grazing removal of record-bearing substrate or variable extension rates are therefore reduced by inter-colony averaging across a study region. We recognize that there is a time and cost tradeoff for applying inter-colony comparisons as a general calibration

strategy. We also recognize that long lived (i.e., multi-century) colonies may be difficult to locate in a given study area, and cores from multiple colonies may not be available for paleoclimate analysis. However, we argue that the benefits of having a more credible climate time series warrant the additional costs and effort when multi-colony work is possible.

Although the assumption of a linear relationship between $\delta^{18}O_{SW}$ and SSS is difficult to constrain, our results suggest that this assumption holds true for this particular study area. We find a weak correlation between SSS and Koror airport precipitation (Tables 3a and 3b), supporting previous conjectures that ocean advection and/or atmospheric evaporation is an important control on regional SSS in the waters surrounding Palau (Morimoto et al., 2002; Grottoli, 2006; Grottoli et al., 2010). We further suggest that SSS is likely to be a greater integrator of regional hydrologic balance than data from any single precipitation station.

Since regressions were performed using monthly anomalies, coefficients a_1 and a_2 differ in magnitude from calibration experiments aimed at determining thermodynamic $^{18}O_{CRL}$-temperature partitioning and $\delta^{18}O_{SW}$–SSS regression. Despite biases associated with serial autocorrelation, we experimented with multiple linear regression models using the original time series for the period 1970–2008 (Appendix Table A.4). The $\delta^{18}O_{CRL}$-SST fractionation slopes range from −0.06 (RI) to −0.14‰/°C (NGB). These values are lower than the generally accepted values of −0.18 to −0.22‰/1 °C increase for *Porites* sp. (Grottoli and Eakin, 2007). In a calibration analysis of *Porites lobata*

Table 3b
Same as in Table 3a for the period 1970 to 2000 ($p < 0.05$). 4 coral refers to the time-averaged composite of BI, UC, RI, and NGB.

|	SSS	SST	Precip.	UC	RI	NGB	BI	4 coral
SSS	1	−0.35	−0.31	0.63	0.62	0.56	0.65	0.75
SST		1	0.25	−0.49	−0.42	−0.58	−0.59	−0.63
Precip.			1	−0.35	−0.39	−0.30	−0.40	−0.44
UC				1	0.61	0.53	0.60	0.82
RI					1	0.48	0.65	0.82
NGB						1	0.57	0.80
BI							1	0.85
4 coral								1

Table 4a
Results of multiple linear regression analyses using monthly anomalies for coral and instrumental data for the period 1970 to 2008. 3 coral refers to the time-averaged composite of UC, RI, and NGB. The 95% confidence bounds for coefficients are shown in parentheses. Pearson's coefficient (r) and p-values between modeled and measured records shown. These data have not been detrended.

SITE	Equation $\delta^{18}O_{ANOM}$ (‰) = a_1 (‰/°C) SST$_{ANOM}$ (°C) + a_2 (‰/psu) SSS$_{ANOM}$ (psu)	r	p
UC	$\delta^{18}O_{ANOM}$ = −0.09 (±0.03) SST + 0.33 (±0.05) SSS	0.61	<0.01
RI	$\delta^{18}O_{ANOM}$ = −0.03 (±0.03) SST + 0.36 (±0.05) SSS	0.57	<0.01
NGB	$\delta^{18}O_{ANOM}$ = −0.15 (±0.03) SST + 0.36 (±0.07) SSS	0.61	<0.01
3 coral	$\delta^{18}O_{ANOM}$ = −0.09 (±0.02) SST + 0.35 (±0.04) SSS	0.75	<0.01

Table 3a
Pearson product–moment correlation matrix between all monthly resolved $\delta^{18}O_{CRL}$ records and instrumental data for the period 1970 to 2008 ($p < 0.05$). 3 coral refers to the time-averaged composite of UC, RI, and NGB.

	SSS	SST	Precip.	UC	RI	NGB	3 coral
SSS	1	−0.40	−0.30	0.65	0.65	0.59	0.74
SST		1	0.27	−0.51	−0.44	−0.57	−0.61
Precip.			1	−0.33	−0.37	−0.28	−0.38
UC				1	0.63	0.56	0.84
RI					1	0.54	0.84
NGB						1	0.85
3 coral							1

Table 4b
Same as in Table 3b for the period 1970–2000. 4 coral refers to the time-averaged composite of BI, UC, RI, and NGB. These data have not been detrended.

SITE	Equation $\delta^{18}O_{ANOM}$ (‰) = a_1 (‰/°C) SST$_{ANOM}$ (°C) + a_2 (‰/psu) SSS$_{ANOM}$ (psu)	r	p
UC	$\delta^{18}O_{ANOM}$ = −0.08 (±0.03) SST + 0.33 (±0.06) SSS	0.59	<0.01
RI	$\delta^{18}O_{ANOM}$ = −0.01 (±0.03) SST + 0.33 (±0.06) SSS	0.51	<0.01
NGB	$\delta^{18}O_{ANOM}$ = −0.13 (±0.04) SST + 0.31 (±0.07) SSS	0.56	<0.01
BI	$\delta^{18}O_{ANOM}$ = −0.09 (±0.03) SST + 0.37 (±0.05) SSS	0.66	<0.01
4 coral	$\delta^{18}O_{ANOM}$ = −0.08 (±0.02) SST + 0.33 (±0.03) SSS	0.77	<0.01
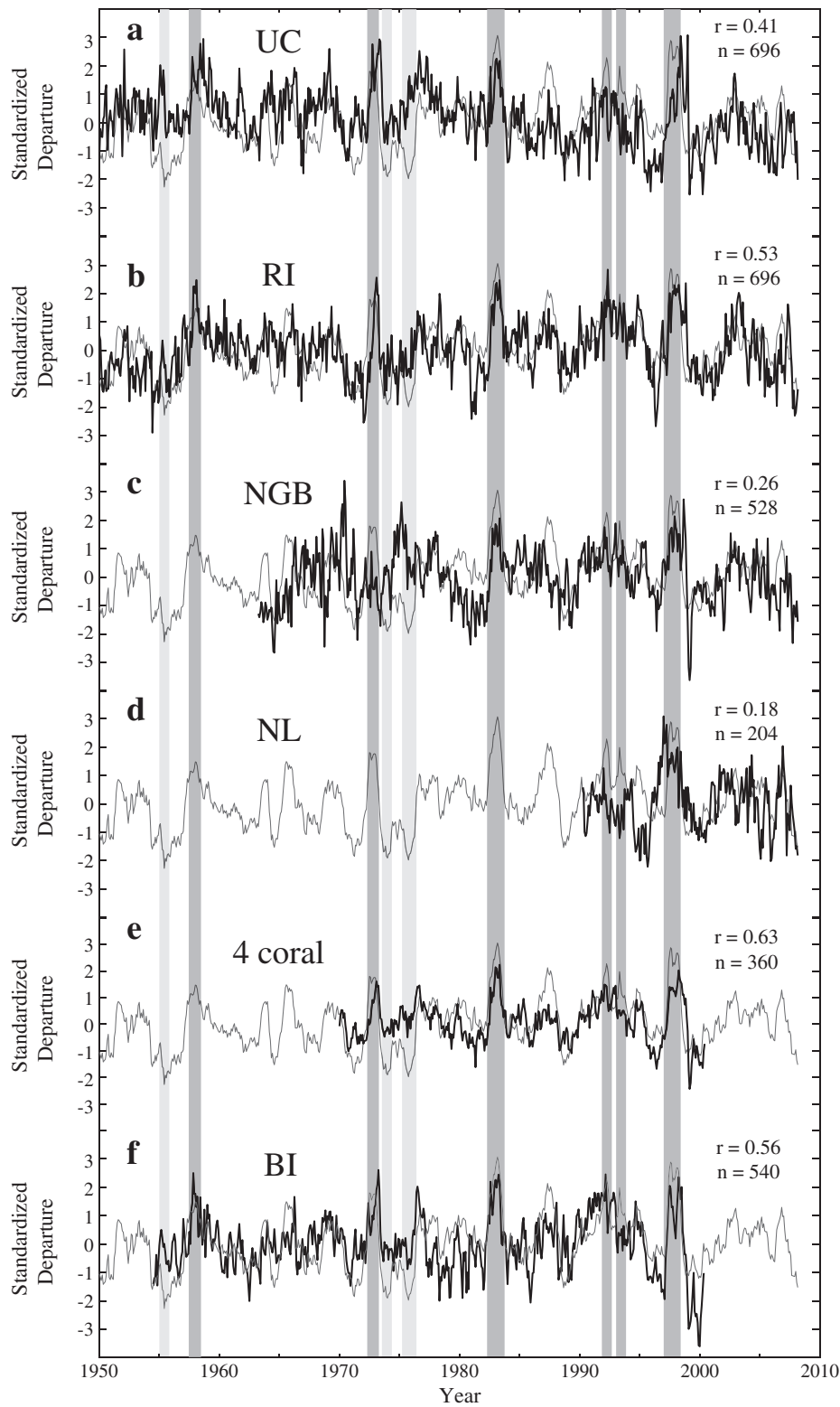
Fig. 7. Detrended $\delta^{18}O$ anomaly records (black) with MEI (gray) for 1950–2008. Correlation coefficient (r) ($p < 0.1$) and samples size (n) are indicated for each record. a) Ulong Channel. b) Rock Islands. c) Ngaragbel. d) Ngeralang. e) 4 coral composite. f) Baebldaob Island (Iijima et al., 2005). Dark (light) shaded regions indicate periods when the MEI shows positive (negative) values exceeding 1.7 standard deviations indicative of ENSO warm (cold) events.

records from Guam, Asami et al. (2004) document similar issues with reduced $\delta^{18}O$–SSS slopes. In their study, they cite four potential factors: 1) small seasonal SST variation, 2) greater contribution of $\delta^{18}O_{SW}$, 3) species dependence, and 4) age model errors. They conclude that high $\delta^{18}O_{SW}$ variability and minimal SST seasonality in Guam results in lower $\delta^{18}O$–SSS slopes and weaker $\delta^{18}O_{CRL}$-SST correlations when

compared to sites with greater SST seasonality and less variable $\delta^{18}O_{SW}$. Our results in Palau support and further this conclusion. The mean SST seasonality in Palau (~1.5 °C) is even less than in Guam (~2.5 °C), and the slopes of our calculated $\delta^{18}O$–SSS regressions are even smaller than those estimated by Asami et al. (2004). Efforts to 're-tune' our age model subannually do not significantly alter this result.

We cannot discount differences in *Porites* species effects, as the corals here are *Porites lutea* while the corals examined by Asami et al. (2004) are *P. lobata*. However, we argue that the more likely cause is the reduced SST seasonality in Palau. An intriguing possibility is that vital effects may be related to seasonality, an issue requiring further investigation. A notable difference between the Guam results and this study is that our $\delta^{18}O_{CRL}$–SSS correlations are higher than $\delta^{18}O_{CRL}$-SST in all instances (Tables 3a, 3b, and 4a, 4b), whereas in Guam the $\delta^{18}O_{CRL}$-SST correlations were greater. Qualitatively, our results suggest that regions with reduced SST variability will have a reduced signal to noise ratio, which poses a challenge for temperature calibration. We also recognize that the relative influences of SSS and SST on $\delta^{18}O_{CRL}$ are non-stationary, and in the pre-instrumental period it may be impossible to disentangle the competing effects of SSS and SST on $\delta^{18}O_{CRL}$ without an independent proxy for either variable. Nonetheless, our $\delta^{18}O_{CRL}$ calibrations provide evidence that the SSS is the dominant control on $\delta^{18}O_{CRL}$ in Palau, a finding that provides context for pre-instrumental paleooceanographic investigations.

5.2. Relationship to ENSO

Fig. 7 shows the $\delta^{18}O_{ANOM}$ for all sites with the MEI. As with Fig. 4, we removed the linear trend and plot the results to unit variance for visual comparison. Note that we chose to include the entire span of each record back to 1950 where possible and the sample size varies between the records. As a result, the correlation coefficients displayed in Fig. 7 should not be compared with one another except in instances where the sample size and record span are similar. In order to draw direct comparisons, we report the δ^{18}O-MEI correlations for the two respective calibration periods (Appendix Table A.5). Overall, there is strong agreement between all of the monthly anomaly time series and the MEI. The results displayed in Fig. 7 further support our conclusion that regional climate forcing and ENSO variability exerts a stronger control on Palau $\delta^{18}O_{CRL}$ than site to site differences. Qualitatively, the anomaly records capture ENSO warm events better than ENSO cool events, an observation relevant to studies seeking to extend the MEI into the pre-instrumental period.

5.3. Interannual, decadal and long term trends

Observational evidence suggests that the WPWP has experienced a slight warming of ~0.5 °C and freshening of 0.1–0.3 psu since 1970 (Delcroix et al., 2007; Grottoli and Eakin, 2007; Cravatte et al., 2009). To assess the long term trends in the Palau $\delta^{18}O_{CRL}$ and instrumental records, we performed linear trend tests for the periods 1970–2008 and 1990–2008 (Appendix Table A.6). The latter period was selected in order to include NL. The NCEP-NCAR SST trend for Palau shows a ~0.7 °C increase for 1970–2008 and a ~0.5 °C increase for 1990–2008, while the LEGOS SSS for Palau shows a freshening of ~0.21 psu for 1970–2008 and a ~0.27 psu for 1990–2008. If we assume $a_1 = -0.19‰/°C$ and $a_2 = 0.42‰/psu$, the cumulative long term trend in $\delta^{18}O_{CRL}$ for 1970–2008 should be ~0.21‰, and the predicted value for 1990–2008 should be ~0.22‰. The magnitude of the long terms trends is therefore equivalent to half of the mean amplitude of the annual cycle (Table 2). All Palau records show decreasing $\delta^{18}O_{CRL}$ during both time intervals. However, the magnitude of trends varies between sites, and in most cases the observed $\delta^{18}O_{CRL}$ trend differs from the predicted values based on instrumental records. For example, the decreasing trend at NGB for 1970–2008 (~0.42‰) is twice the predicted value of ~0.21‰. Conversely, RI shows no statistically significant trend during this interval. For the period 1970–2008, the UC record displays the best predictive skill. For the latter period 1990–2008, the RI trend (~0.23‰) displays the greater predictive skill, UC displays no significant trend, and both NL (~0.26‰) and NGB (~0.35‰) overestimate the predicted effect on $\delta^{18}O_{CRL}$. For both time intervals the 3 coral composite has the greatest

overall predictive skill. We conclude from these analyses that the long term trends are consistent with modern observations of warming and freshening, but the linear trends from individual sites within Palau should be interpreted with caution. However, the greater predictive skill of the 3 coral composite further demonstrates the utility of using time-averaged $\delta^{18}O_{CRL}$ records from distributed sites (Linsley et al., 1999).

In order to inspect interannual and interdecadal trends in the Palau records, we applied a 1.1 year low pass filter to each of the Palau $\delta^{18}O_{CRL}$ records (Fig. 8). In contrast to the long term trends at individual sites, the records display coherency at interannual to decadal time scales. Interannual variability is generally greater after ~1970, though longer records from Palau will be necessary to evaluate the significance of decadal and interdecadal trends. The coherency of records on interannaul and interdecadal time scales provides confidence that longer records will reveal key features of climate variability in the pre-instrumental period. Overall our results suggest that Palau coral records are well suited to address questions of
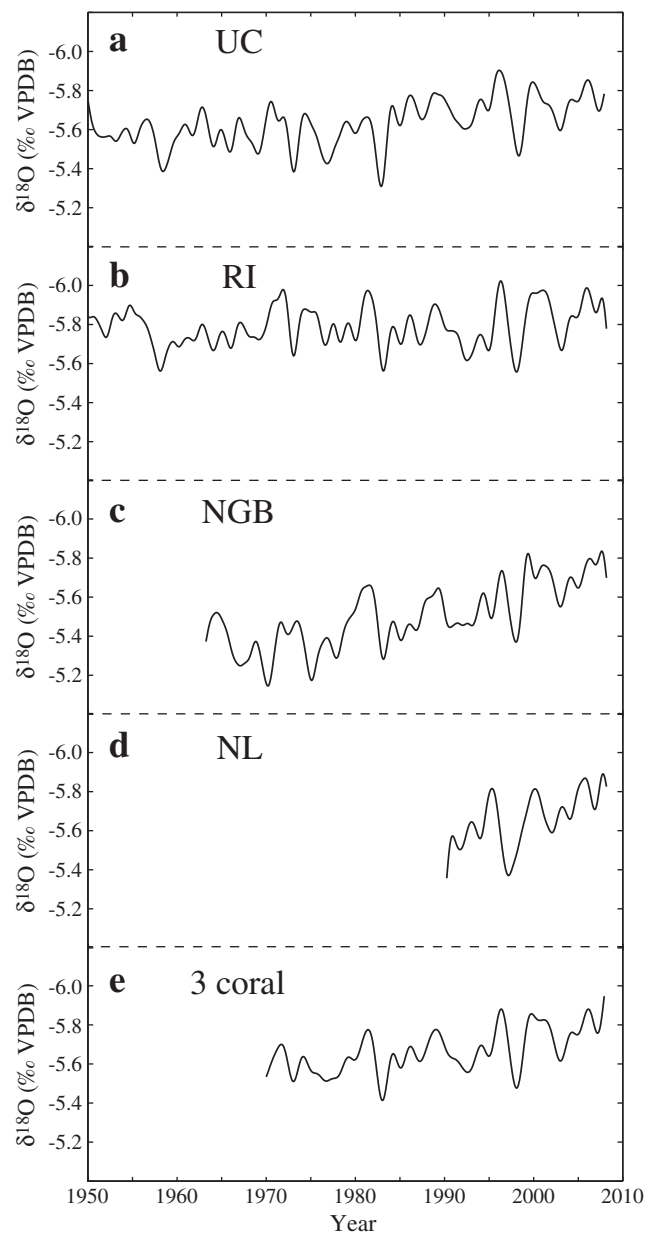

Fig. 8. Time series of Palau δ^{18}O records after applying a 1.1 year low pass filter. a) Ulong Channel. b) Rock Islands. c) Ngaragbel. d) Ngeralang.

multi-decadal to centennial climate variability in this important region of the WPWP, particularly in relation to ENSO variability. The present study establishes a calibration framework that can be applied to records from the pre-instrumental period. Such long term records are essential for assessing the significance of recent WPWP warming and freshening trends in this sector of the climate system.

Supplementary data to this article can be found online at http://dx.doi.org/10.1016/j.palaeo.2013.06.001.

References

Asami, R., Yamada, T., Iryu, Y., Meyer, C.P., Quinn, T.M., Paulay, G., 2004. Carbon and oxygen isotopic composition of a Guam coral and their relationships to environmental variables in the western Pacific. Palaeogeography, Palaeoclimatology, Palaeoecology 212, 1–22.

Asami, R., Yamada, T., Iryu, Y., Quinn, T.M., Meyer, C.P., Paulay, G., 2005. Interannual and decadal variability of the western Pacific sea surface condition for the years 1787–2000: reconstruction based on stable isotope record from a Guam coral. Journal of Geophysical Research 110, C05018.

Brown, J., Tudhope, A.W., Collins, M., McGregor, H.V., 2008. Mid-Holocene ENSO: issues in quantitative model-proxy data comparisons. Paleoceanography 23, PA3202.

Bruno, J., Siddon, C., Witman, J., Colin, P., Toscano, M., 2001. El Niño related coral bleaching in Palau, Western Caroline Islands. Coral Reefs 20, 127–136.

Carton, J.A., Giese, B.S., 2008. A reanalysis of ocean climate using Simple Ocean Data Assimilation (SODA). Monthly Weather Review 136, 2999–3017.

Chen, D., Cane, M.A., Kaplan, A., Zebiak, S.E., Huang, D., 2004. Predictability of El Niño over the past 148 years. Nature 428, 733–736.

Cobb, K.M., Charles, C.D., Cheng, H., Edwards, R.L., 2003. El Niño/Southern Oscillation and tropical Pacific climate during the last millennium. Nature 424, 271–276.

Cohen, A.L., McConnaughey, T.A., 2003. Geochemical perspectives on coral mineralization. Reviews in Mineralogy and Geochemistry 54, 151–187.

Cole, J.E., Fairbanks, R.G., Shen, G.T., 1993. Recent variability in the Southern Oscillation: isotopic results from a Tarawa Atoll coral. Science 260, 1790–1793.

Colin, P., 2009. Marine Environments of Palau. Indo-Pacific Press, San Diego, CA 414.

Collins, M., An, S.-I., Cai, W., Ganachaud, A., Guilyardi, E., Jin, F.-F., Jochum, M., Lengaigne, M., Power, S., Timmermann, A., Vecchi, G., Wittenberg, A., 2010. The impact of global warming on the tropical Pacific Ocean and El Niño. Nature Geoscience 3, 391–397.

Corrège, T., 2006. Sea surface temperature and salinity reconstruction from coral geochemical tracers. Palaeogeography, Palaeoclimatology, Palaeoecology 232, 408–428.

Cravatte, S., Delcroix, T., Zhang, D., McPhaden, M., Leloup, J., 2009. Observed freshening and warming of the western Pacific Warm Pool. Climate Dynamics 33, 565–589.

Delcroix, T., Cravatte, S., McPhaden, M.J., 2007. Decadal variations and trends in tropical Pacific sea surface salinity since 1970. Journal of Geophysical Research 112, C03012.

Delcroix, T., Alory, G., Cravatte, S., Corrège, T., McPhaden, M.J., 2011. A gridded sea surface salinity data set for the tropical Pacific with sample applications (1950–2008). Deep Sea Research Part I: Oceanographic Research Papers 58, 38–48.

Dunbar, R.B., Cole, J.E., 1999. Annual records of tropical systems (ARTS). Pages Workshop Report, Series 99–1. (72 pp.).

Dunbar, R.B., Wellington, G.M., Colgan, M.W., Glynn, P.W., 1994. Eastern Pacific sea surface temperature since 1600 A.D.: the $\delta^{18}O$ record of climate variability in Galápagos corals. Paleoceanography 9 (2), 291–315.

Durack, P.J., Wijffels, S.E., 2010. Fifty-year trends in global ocean salinities and their relationship to broad-scale warming. Journal of Climate 23, 4342–4362.

Durack, P.J., Wijffels, S.E., Matear, R.J., 2012. Ocean salinities reveal strong global water cycle intensification during 1950 to 2000. Science 336, 455–458.

Evans, M.N., Kaplan, A., Cane, M.A., 2002. Pacific sea surface temperature field reconstruction from coral $\delta^{18}O$ data using reduced space objective analysis. Paleoceanography 17, 1007.

Fairbanks, R.G., Evans, M.N., Rubenstone, J.L., Mortlock, R.A., Broad, K., Moore, M.D., Charles, C.D., 1997. Evaluating climate indices and their geochemical proxies measured in corals. Coral Reefs 16, 93–100.

Felis, T., Pätzold, J., Loya, Y., 2003. Mean oxygen-isotope signatures in Porites spp. corals: inter-colony variability and correction for extension-rate effects. Coral Reefs 22, 328–336.

Fine, R.A., Lukas, R., Bingham, F.M., Warner, M.J., Gammon, R.H., 1994. The western equatorial Pacific: a water mass crossroads. Journal of Geophysical Research 99, 25063–25080.

Gagan, M.K., Ayliffe, L.K., Beck, J.W., Cole, J.E., Druffel, E.R.M., Dunbar, R.B., Schrag, D.P., 2000. New views of tropical paleoclimates from corals. Quaternary Science Reviews 19, 45–64.

Gorman, M.K., Quinn, T.M., Taylor, F.W., Partin, J.W., Cabioch, G., Austin Jr., J.A., Pelletier, B., Ballu, V., Maes, C., Saustrup, S., 2012. A coral-based reconstruction of sea surface salinity at Sabine Bank, Vanuatu from 1842 to 2007 CE. Paleoceanography 27, PA3226.

Graham, N.E., Barnett, T.P., 1987. Sea surface temperature, surface wind divergence, and convection over tropical oceans. Science 238, 657–659.

Grottoli, A.G., 2006. Monthly resolved stable oxygen isotopes in a Palauan sclerosponge Acanthocheates wellsi for the period 1977–2001. Proceedings of the 10th International Coral Reef Symposium, Okinawa, Japan, pp. 572–579.

Grottoli, A.G., Eakin, C.M., 2007. A review of modern coral $\delta^{18}O$ and $\Delta^{14}C$ proxy records. Earth-Science Reviews 81, 67–91.

Grottoli, A.G., Adkins, J.F., Panero, W.R., Reaman, D.M., Moots, K., 2010. Growth rates, stable oxygen isotopes ($\delta^{18}O$), and strontium (Sr/Ca) composition in two species of Pacific sclerosponges (Acanthocheatetes wellsi and Astrosclera willeyana) with $\delta^{18}O$ calibration and application to paleoceanography. Journal of Geophysical Research 115, C06008.

Guilderson, T.P., Schrag, D.P., 1999. Reliability of coral isotope records from the western Pacific warm pool: a comparison using age-optimized records. Paleoceanography 14, 457–464.

Hendy, E.J., Gagan, M.K., Alibert, C.A., McCulloch, M.T., Lough, J.M., Isdale, P.J., 2002. Abrupt decrease in tropical Pacific sea surface salinity at end of Little Ice Age. Science 295, 1511–1514.

Heron, S., Joseph Metzger, E., Skirving, W., 2006. Seasonal variations of the ocean surface circulation in the vicinity of Palau. Journal of Oceanography 62, 413–426.

Iijima, H., Kayanne, H., Morimoto, M., Abe, O., 2005. Interannual sea surface salinity changes in the western Pacific from 1954 to 2000 based on coral isotope analysis. Geophysical Research Letters 32, L04608.

Juillet-Leclerc, A., Reynaud, S., Rollion-Bard, C., Cuif, J.P., Dauphin, Y., Blamart, D., Ferrier-Pagès, C., Allemand, D., 2009. Oxygen isotopic signature of the skeletal microstructures in cultured corals: identification of vital effects. Geochimica et Cosmochimica Acta 73, 5320–5332.

Kalnay, E., Kanamitsu, M., Kistler, R., Collins, W., Deaven, D., Gandin, L., Iredell, M., Saha, S., White, G., Woollen, J., Zhu, Y., Leetmaa, A., Reynolds, R., Chelliah, M., Ebisuzaki, W., Higgins, W., Janowiak, J., Mo, K.C., Ropelewski, C., Wang, J., Jenne, R., Joseph, D., 1996. The NCEP/NCAR 40-year reanalysis project. Bulletin of the American Meteorological Society 77, 437–471.

Krief, S., Hendy, E.J., Fine, M., Yam, R., Meibom, A., Foster, G.L., Shemesh, A., 2010. Physiological and isotopic responses of scleractinian corals to ocean acidification. Geochimica et Cosmochimica Acta 74, 4988–5001.

LeGrande, A.N., Schmidt, G.A., 2006. Global gridded data set of the oxygen isotopic composition in seawater. Geophysical Research Letters 33, L12604.

Linsley, B.K., Messier, R.G., Dunbar, R.B., 1999. Assessing between-colony oxygen isotope variability in the coral Porites lobata at Clipperton Atoll. Coral Reefs 18, 13–27.

Linsley, B.K., Zhang, P., Kaplan, A., Howe, S.S., Wellington, G.M., 2008. Interdecadal–decadal climate variability from multicoral oxygen isotope records in the South Pacific Convergence Zone region since 1650 A.D. Paleoceanography 23, PA2219.

Maes, C., Picaut, J.I., Belamari, S., 2005. Importance of the salinity barrier layer for the Buildup of El Niño. Journal of Climate 18, 104–118.

McConnaughey, T.A., 2003. Sub-equilibrium oxygen-18 and carbon-13 levels in biological carbonates: carbonate and kinetic models. Coral Reefs 22, 316–327.

Millero, F.J., Feistel, R., Wright, D.G., McDougall, T.J., 2008. The composition of standard seawater and the definition of the reference-composition salinity scale. Deep Sea Research Part I: Oceanographic Research Papers 55, 50–72.

Mizrachi, I., Loya, Y., Rosenfeld, M., Kramarski-Winter, E., Yam, R., Shemesh, A., 2010. The build up of the isotopic signal in skeletons of the stony coral Porites lutea. Geochimica et Cosmochimica Acta 74, 7021–7030.

Morimoto, M., Abe, O., Kayanne, H., Kurita, N., Matsumoto, E., Yoshida, N., 2002. Salinity records for the 1997–98 El Niño from Western Pacific corals. Geophysical Research Letters 29, 31–34.

Picaut, J., Ioualalen, M., Menkes, C., Delcroix, T., McPhaden, M.J., 1996. Mechanism of the zonal displacements of the Pacific warm pool: implications for ENSO. Science 274, 1486–1489.

Quinn, T.M., Sampson, D.E., 2002. A multiproxy approach to reconstructing sea surface conditions using coral skeleton geochemistry. Paleoceanography 17, 1062.

Quinn, T.M., Crowley, T.J., Taylor, F.W., Henin, C., Joannot, P., Join, Y., 1998. A Multicentury stable isotope record from a New Caledonia coral: Interannual and decadal sea surface temperature variability in the southwest Pacific since 1657 A.D. Paleoceanography 13, 412–426.

Rosenheim, B.E., Swart, P.K., 2007. Caribbean sclerosponge radiocarbon measurements re-interpreted in terms of U/Th age models. Nuclear Instruments and Methods in Physics Research Section B: Beam Interactions with Materials and Atoms 259, 474–478.

Sinclair, D.J., 2005. Correlated trace element "vital effects" in tropical corals: a new geochemical tool for probing biomineralization. Geochimica et Cosmochimica Acta 69, 3265–3284.

Stephans, C.L., Quinn, T.M., Taylor, F.W., Corrège, T., 2004. Assessing the reproducibility of coral-based climate records. Geophysical Research Letters 31, L18210.

Swart, P.K., Moore, M., Charles, C., Böhm, F., 1998. Sclerosponges may hold new keys to marine paleoclimate. Eos 79, 633–636.

Thompson, D.M., Ault, T.R., Evans, M.N., Cole, J.E., Emile-Geay, J., 2011. Comparison of observed and simulated tropical climate trends using a forward model of coral $\delta^{18}O$. Geophysical Research Letters 38, L14706.

Tudhope, A.W., Shimmield, G.B., Chilcott, C.P., Jebb, M., Fallick, A.E., Dalgleish, A.N., 1995. Recent changes in climate in the far western equatorial Pacific and their relationship to the Southern Oscillation; oxygen isotope records from massive corals, Papua New Guinea. Earth and Planetary Science Letters 136, 575–590.

Urban, F.E., Cole, J.E., Overpeck, J.T., 2000. Influence of mean climate change on climate variability from a 155-year tropical Pacific coral record. Nature 407, 989–993.

Weber, J.N., Woodhead, P.M.J., 1972. Temperature dependence of oxygen-18 concentration in reef coral carbonates. Journal of Geophysical Research 77, 463–473.

Wolankski, E., Furukawa, K., 2007. The oceanography of Palau. In: Kayane, H., Omori, M., Fabricus, K., Verheij, E., Colin, P., Golbuu, Y., Yukihira, H. (Eds.), Coral Reefs of Palau. Palau International Coral Reef Center, Palau, pp. 59–72.

Wolter, K., Timlin, M.S., 1993. Monitoring ENSO in COADS with a seasonally adjusted principal component index. Proceedings of the 17th Climate Diagnostics Workshop, Norman, OK, NOAA/NMC/CAC, NSSL, Oklahoma Climate Survey, SIMMS and the School of Meteor., Univ. of Oklahoma, pp. 52–57.

Wolter, K., Timlin, M.S., 1998. Measuring the strength of ENSO events — how does 1997/98 rank? Weather 53, 315–324.

Wolter, K., Timlin, M.S., 2011. El Niño/Southern Oscillation behaviour since 1871 as diagnosed in an extended Multivariate ENSO index (MEI.ext.). International Journal of Climatology 31, 1074–1087.

Wu, H., Grottoli, A., 2010. Stable oxygen isotope records of corals and a sclerosponge in the western Pacific warm pool. Coral Reefs 29, 413–418.

Wyrtiki, K., 1989. Some thoughts about the west Pacific warm pool. Proceedings of the Western Pacific International Meeting and Workshop on TOGA COARE, Nouméa, New Caledonia, pp. 99–109.

Xie, P., Arkin, P.A., 1997. Global precipitation: a 17-year monthly analysis based on gauge observations, satellite estimates, and numerical model outputs. Bulletin of the American Meteorological Society 78, 2539–2558.